RASĀYAN *J. Chem.*
Vol. 19 | No. 3 | 1539-1552 | July-September | 2026
ISSN: 0974-1496 | e-ISSN: 0976-0083 | CODEN: RJCABP
http://www.rasayanjournal.com
http://www.rasayanjournal.co.in

LOW-TEMPERATURE GREEN PREPARATION OF OXYGEN FUNCTIONALIZED GRAPHITIC CARBON NITRIDE FOR SELECTIVE FLUORESCENCE SENSING OF CHROMIUM (VI) IONS IN TANNERY EFFLUENT AND FOOD SAMPLES

C. Valarmathy and S. Sudhaparimala✉
Post Graduate and Research Department of Chemistry, Ethiraj College for Women, University of Madras, Chennai-600008, Tamil Nadu, India
✉Corresponding author: sudhaparimala_s@ethirajcollege.edu.in

ABSTRACT

Graphitic Carbon Nitride (GCN) has gained value in the field of sensors due to its unique electronic band structure and electron transfer characteristics, resulting in improved fluorescent properties. Functionalizing the surface of GCN with heteroatoms enables selective sensing of the target analyte. Thus, the present study involves the preparation of Oxygen-functionalized GCN from the urea and aqueous extract of the leaves of *Moringa oleifera* through a simple, low-temperature thermal carbonisation method. The microstructure, chemical functionalities, surface-active principles, and surface morphology of the prepared GCN were studied extensively using spectroscopic and microscopic tools. The fluorescence activity of the prepared GCN was analysed with respect to all significant experimental parameters, and its behaviour was further explored for selective sensing of heavy metal ions. The prepared GCN exhibited a lower detectable limit of 59 µM towards sensing of Chromium (VI) ions, and was successfully applied for detecting Cr (VI) ions as pollutants in tannery industrial effluent and adulterants in commercial food-grade turmeric powders. The study contributes to the sustainable field of nanotechnology by developing a simple, economical, and energy-efficient low-temperature method for the preparation of functionalized GCN. The path forward of the present study will be to focus on tuning the surface chemistry of the prepared GCN to achieve improved sensitivity and broader applicability in environmental and biomedical monitoring. Ultimately, the study highlights the potential of eco-friendly precursors in developing advanced functional nano sensors for detecting Cr (VI) in industrial effluents, which matches with the Sustainable Development Goal-6 (SDG-6).

Keywords: Graphitic Carbon Nitride, Heavy Metal Ion, *Moringa Oleifera,* Fluorescence Sensor, And Quenching of Fluorescence.

RASĀYAN *J. Chem.*, Vol. 19, No. 3, 2026

INTRODUCTION

Graphitic Carbon Nitride (GCN) has emerged as a promising metal-free semiconductor due to its unique electronic structure, chemical stability, and visible-light absorption behavior.[1] The strong π-conjugated structure of the GCN facilitates very good electron transfer characteristics, leading to excellent thermochemical stability and fluorescence property.[2,3] The incorporation of non-metal heteroatoms such as Oxygen into the surface of the GCN (functionalized GCN) extends the light absorption range, increases the surface area, and reduces the electron-hole recombination rate.[4,5] The functionalization of GCN leads to an altered electronic structure, resulting in improved fluorescent properties and enhanced surface-active sites that can be tapped for application studies, especially in sensors.[6] The Graphitic Carbon Nitride is widely prepared through methods such as liquid phase exfoliation, chemical oxidation, hydrothermal method, and thermal method (pyrolysis).[7] Among these, the one-step thermal condensation of nitrogen-rich precursors such as urea, melamine, dicyanamide, cyanamide and thiourea at different temperatures is the most widely used method.[1] The reported studies state that the GCN preparatory methods are generally energy-intensive, thereby requiring high temperatures in the range of 500°C-700°C.[8] An important research gap remains in developing a low-temperature (<400°C) synthesis route for the preparation of functionalized GCN without losing its structural integrity and functional performance. It is important to address this existing research gap in order to scale up the sustainable production of GCN-based advanced functional materials. Urea is a commonly used precursor for the preparation of GCN due to its low cost,

availability, and well-defined thermal decomposition pathway. On subjecting urea to thermal carbonisation, it leads to the formation of melamine through intermediates such as isocyanic acid and cyanuric acid. The melamine then undergoes polymerisation to form the GCN structural network.[9] Tailoring the surface properties (functionalization) of GCN using bio-precursors has gained significant attention in recent research. The leaves of *Moringa Oleifera* (MO) are rich in organic bioactive phytochemicals such as tannins, flavonoids, polyphenolic acids, and proteins.[10,11] Upon thermal treatment, these bioactive phytochemicals decompose into smaller heterocyclic compounds, enabling effective surface functionalization of GCN with heteroatoms.[12,13] Hexavalent chromium [Cr (VI)] is a highly toxic pollutant widely released from electroplating, textile, and leather industries.[14] Its presence in ecological systems, specifically the water and food systems, poses severe health risks, including carcinogenic and mutagenic effects to human health. Hence, the rapid and sensitive detection of Cr (VI) ions in ecosystems is very important.[15] The advanced analytical techniques like Atomic Absorption spectroscopy (AAS), Inductively Coupled Plasma Optical Emission Spectroscopy (ICP-OES) & Inductively Coupled Plasma Mass Spectroscopy (ICP-MS) are often expensive, time-consuming, and require sophisticated instrumentation. In recent days, fluorescence-based sensing has emerged as a simple, rapid, highly sensitive, and selective alternative method.[16] Specifically, GCN with a well-defined two-dimensional layered structure, a suitable band gap energy (2.7 eV) and tunable surface functional groups offers excellent potential as a fluorescent sensor.[4] The surface functionalities, such as hydroxyl, carbonyl, and amine groups, play an important role in enhancing selectivity toward target analytes such as Cr (VI) ions.[17] The present study aims to address the existing research gap by developing a low-temperature (<400°C) method for the preparation of Oxygen-functionalized GCN using urea and aqueous extract of the leaves of *Moringa oleifera.* The study also evaluates the performance of the prepared functionalized GCN as a selective fluorescent sensor for the rapid and reliable detection of Cr (VI) ions. The present study matches with the Sustainable Development Goal 3: Good Health and Well-being, by focusing on the development of an economical and efficient sensor for the detection of toxic heavy metal ions that pose serious risks to human health. By rapidly monitoring the presence of Cr (VI) ions in environmental and food systems, the present study contributes toward improving public health safety and reducing exposure to hazardous contaminants.

EXPERIMENTAL

Material and Methods

The fresh leaves of *Moringa Oleifera* were collected from an interior rural place (Gummidipoondi) in the Tiruvallur district of Tamil Nadu, India. The collected plant leaves were authenticated by the Botanical Survey of India, Southern Regional Centre, Government of India (REF. NO. BSI/SRC/5/23/2024-25/TECH./374). For the synthesis of GCN, urea was purchased from Nice Chemicals and used as received. Deionised water was used for the experiments. The heavy metal salts that were used to screen the selectivity of the prepared GCN towards sensing were Zinc sulfate (Nice Chemicals), Calcium chloride (Nice chemicals), Cadmium carbonate (Nice chemicals), Magnesium sulfate (Nice chemicals), Barium chloride (Molychem), Manganese chloride (Spectrum), Ferrous sulfate (Nice chemicals), Ferric chloride (Nice chemicals), Chromic potassium sulfate (Nice chemicals), Arsenic trioxide (Molychem), Cobalt sulfate (Nice chemicals), Nickel chloride (Fine-chem), Lead acetate (Molychem), Copper sulfate (Molychem), Mercuric chloride (Spectrum), and Potassium dichromate (Qualigens). The real-time application study was extended to detect the Cr (VI) ions in industrial effluents and food samples. Based on the reports, the tannery industrial effluent was simulated using Sodium acetate (Isochem), Ammonium chloride (Isochem), monosodium phosphate (Emplura), Magnesium sulfate (Nice Chemicals), Cadmium carbonate (Nice Chemicals), Copper sulphate (Molychem), Lead acetate (Molychem), Potassium dichromate (Molychem), and Zinc sulphate (Nice Chemicals). Three different varieties (one branded, one locally branded, and one unbranded) of commercial food-grade turmeric powders were purchased from the local market in Gummidipoondi, Tamil Nadu. All the chemicals were used as received.

Preparation of Oxygen Functionalized Graphitic Carbon Nitride (GCN)

The collected leaves were washed to remove dirt and impurities, then shade-dried and ground into a fine powder. The aqueous extract of the leaves of *Moringa oleifera* was prepared by stirring the dried leaf

powder with water in a ratio of 1/10 (w/v) on a magnetic stirrer at 40°C for 15 minutes.[18] The extract was filtered through a Whatman no.1 filter paper, and the aqueous filtrate was further used for the preparation of GCN. The urea was mixed with the aqueous extract of the leaves of *Moringa oleifera* (10% (w/v) and pH 5.6 (intrinsic pH of the extract)) in the ratio of 0.1g/ml (w/v). The mixture was then subjected to thermal carbonisation at a temperature of 200°C for about four hours in a Hot air oven, resulting in the formation of brownish-yellow solid powder.[19] The processing temperature was fixed based on the thermal decomposition temperature of all the bioactive phytochemicals present in the leaves of *Moringa oleifera.*[11,20]

Structural Analysis

The presence of heteroatoms and their chemical functionalities in the prepared GCN was determined using Fourier-Transform Infrared analysis (*IR Affinity-1*) and X-ray Photoelectron Spectroscopy (XPS) (*Ulvac-Phi*, Inc.; Model: PHI5000 Version Probe III). The surface morphology was confirmed through a High Resolution - Transmission Electron Microscope (*Joel*) image. The microstructural properties, viz.: the number of layers and amount of defect density of the as-prepared GCN, were determined from the Powder X-ray Diffractogram (PXRD) data using a Cu-Kα radiation (*PAN analytical model Xpert Pro*), and the Micro-Raman Spectra recorded using a Micro-Raman spectrometer (*Bruker,* RFS), respectively. The optical properties of the GCN were investigated using absorption (*UV-SHIMADZU 1601*) and emission (fluorescence) (*Agilent, Cary Eclipse*) spectra. The lifetime analysis of the aqueous GCN solution was carried out using the Horiba *Jobin Yvon-Fluorolog F3-111*. The thermal stability of the prepared GCN was assessed by performing thermal analysis using a *NETZSCH STA 2500* TGA-DTA setup.

Screening of Fluorescence Behaviour

The fluorescence behaviour of the prepared GCN was evaluated at various excitation wavelengths (λ_{ex} = 330-355 nm). The concentration-dependent and pH-dependent fluorescent behaviour of the GCN was further analysed by carrying out the fluorescence spectral studies at various concentrations of GCN solutions (250 ppm, 500 ppm, 750 ppm, and 1000 ppm) and at different pH (3, 5, 7, 9, and 11) conditions, respectively. The pH conditions were varied using acetic acid and ammonia solution. The photostability, which is a significant factor, was also investigated by recording the fluorescence spectra of the prepared GCN solution under a UV source for 120 minutes.

Evaluation of the Prepared GCN as an Efficient Fluorescent Sensor

Based on the results of the study, the fluorescence behaviour of the prepared GCN was further extended to detect the presence of heavy metal ions. The selectivity of the prepared GCN towards sensing of heavy metal ions was studied by monitoring the emission intensity of the GCN solution in the presence of sixteen different metal ions (each 10mM) in the ratio of 1:3 (v/v) at an excitation wavelength of 350 nm. The excitation wavelength was fixed based on the maximum emission intensity of the GCN solution and the UV-Visible absorption wavelength of Chromium [Cr (VI)] ions. The sensing efficiency of the prepared GCN towards Chromium [Cr (VI)] ions was further studied at different metal ion concentrations. The influence of pH on the sensing process was analysed at three different pH levels (pH=3, 7 and 11).

Detection of Cr (VI) Ions in Tannery Industrial Effluent and Commercial Food-Grade Turmeric Powders

Chromium metal is widely used in the leather industry for the tanning process. Due to its high solubility in water, the Cr (VI) ions easily get discharged as a pollutant in the industrial effluents, which causes adverse health effects to living beings. The detection and removal of Chromium (VI) ions from the tannery industrial effluent have several difficulties due to the presence of several other chemicals used in the tanning process.[21.] Turmeric is one of the commonly used spices in a variety of food items and is also valued for its medicinal properties. The commercial turmeric powders are often adulterated with toxic chemicals like metanil yellow dye and lead chromate to enhance their colour appearance.[22] Exposure to these synthetic dyes and heavy metals is highly carcinogenic in nature. Hence, it is important to evaluate the adulteration of Cr (VI) ions in the commercial turmeric powders. Therefore, as a preliminary screening study, the present study aims to detect the presence of Cr (VI) ions in tannery industrial effluent

and commercial food-grade turmeric powders. As per the reports of *M. Chowdhury et al.* (2015), the tannery industrial effluent was simulated by mixing all the chemicals used for the process of leather tanning.[23] It was done by mixing Chromium (VI) ions of a total concentration of 1 g/L (w/v) with Sodium acetate, Ammonium chloride, monosodium phosphate, Magnesium nitrate, Cadmium chloride, Copper sulphate, Lead nitrate, and Zinc sulphate. Three different retail turmeric samples (One highly branded, one locally available branded, and one unbranded) were purchased from a local market located in Gummidipoondi taluk, Tiruvallur district, Tamil Nadu, India. Based on the detectable limit of Cr (VI) ions by the prepared GCN, the turmeric sample solution was prepared for the detection of Chromium (VI) contamination. The collected turmeric samples were dissolved in hot water in the ratio of 1:10 (w/v) and then filtered to remove the residue. The aqueous solution of the prepared GCN at a concentration of 0.5 mg/mL (w/v) was added to the tannery industrial effluent and turmeric solution individually in a 3:1 (v/v) ratio, respectively. The fluorescence spectra were recorded immediately after mixing the sample solution with the industrial effluent and turmeric solution at an excitation wavelength of 350 nm. The experiment was performed in triplicate to ensure its repeatability. The concentration of Chromium (VI) ions in real-time samples was determined by constructing a calibration graph (fluorescence intensity Vs known concentration of Cr (VI) ions) using Chromium (VI) ion solutions of known concentration. The results of the fluorescence study were correlated with the ICP-OES results.

RESULTS AND DISCUSSION

Structural Characterization of the Prepared Oxygen-Functionalized GCN

The presence of a broad peak at 2θ of 27.8° in the PXRD pattern of the prepared GCN (Fig.-1a) suggests the formation of (002) graphitic lattice plane with layered structure.[24,25] The diffraction pattern of the prepared GCN matches well with the PXRD pattern of the GCN prepared using urea by *Y. Zhang et al.*[26] The diffraction peak at 10.7° indexed to the (001) plane indicates that the layers in the as-prepared GCN are dispersed with an inter-layer spacing (d-spacing) value of 0.8262 nm. The significantly higher inter-planar spacing compared to that of graphite (0.3353 nm) suggests that the surface of the prepared GCN is enriched with Oxygen-containing functional groups.[27] The intercalation of Oxygen functional groups between the lattice planes in the GCN may be due to the phenolic components, such as flavonoids and phenolic acids, present in the leaves of *Moringa Oleifera.*[11] The absence of the (100) plane indicates the possible dominance of triazine ring units in the prepared GCN structure.[28] From the calculated thickness (D) and the interlayer spacing (d), it is confirmed that the prepared material is a few-layered Graphitic Carbon Nitride (No. of layers = 5) with Oxygen functional groups on its surface. The presence of the D band, G band, and 2D band in the Micro-Raman spectrum of the prepared GCN (Fig.-1b) was observed at 1347 cm^{-1}, 1588 cm^{-1}, and 2857 $cm^{-1,}$ respectively.[18] The identification of the D band (disorder band) indicates the presence of heteroatoms of Oxygen and Nitrogen in the as-prepared GCN. The shift in the position of the G band to a higher wavelength confirms the functionalization of the prepared GCN.[29] The defect density ratio (I_D/I_G) of 0.9913 suggests the presence of almost equal amounts of sp^3 and sp^2 Carbon, which can be due to the presence of triazine-based structural units. The higher defect density ratio correlates with the higher d-spacing from PXRD, which confirms the structurally defective and functionalized nature of the prepared GCN. The appearance of the 2D band confirms the layered structure of the prepared GCN. The shift in 2D band position from 2700 cm^{-1} to 2857 cm^{-1} supports the formation of few-layered GCN, which also correlates well with the PXRD analysis.[30]

The UV-visible spectrum of the GCN (Fig.-1c) exhibits an absorption band at 213 nm and 421 nm due to the π-π^* and n-π^* transitions, respectively. These electronic transitions may be raised due to the presence of sp^2 hybridized Carbon structural network and heteroatoms such as Nitrogen and Oxygen (C=N and C=O), respectively. The presence of the C=N and C=O bonds in the structure of the prepared GCN may be due to the triazine-based structural units and the Oxygen functionalities.[31] The indirect band gap energy of the prepared GCN was determined to be 2.5 eV through the *Tauc's* plot (Inset in Fig.-1c) method. The band gap energy of the prepared GCN falls in the range of semiconductors (0.5 eV to 3.0 eV), which assures enhanced visible light absorption and fluorescence behaviour – key requirements for efficient sensing performance. The FT-IR spectrum of the prepared GCN (Fig.-1d) shows the presence of

a broad peak at 3188 cm^{-1} corresponding to the stretching vibration of amino (N-H) groups and hydroxyl groups in the as-prepared sample.

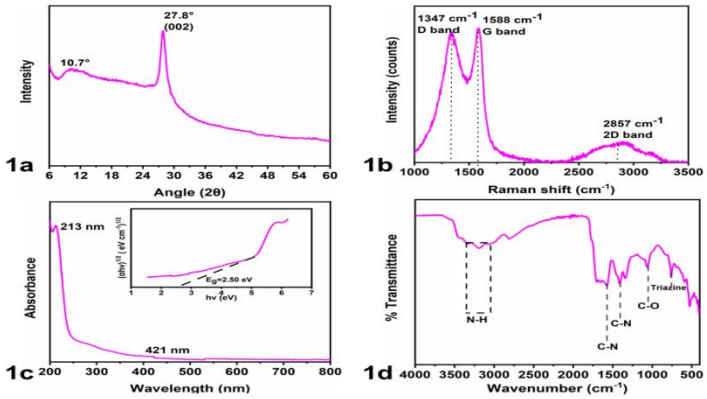

Fig.-(1a) PXRD Pattern, (1b) Micro-Raman, (1c) UV-visible (Inset: *Tauc's* plot), and (1d) FT-IR Spectra of the as-Prepared GCN

The peaks at 1572 cm^{-1} and 1412 cm^{-1} occur due to the C-N stretching in aromatic heterocycles, confirming the formation of carbon nitride. The C-O stretching peak at 1060 cm^{-1} confirms the presence of Oxygen functional groups, correlating with the higher d-spacing and D band (indicative of structural defects) in PXRD and Micro-Raman, respectively. The peak observed at 806 cm^{-1} is characteristic of the triazine ring structure, suggesting that it may be the building block for the as-prepared GCN.[9] The FT-IR spectrum of the prepared sample correlates well with the GCN prepared from Urea and Melamine by *Y. Zheng et al.*[32] The structural (PXRD and Micro-Raman), chemical (FT-IR), and optical (UV-Visible) analyses show that the low-temperature and bio-assisted preparation of functionalized GCN not only retains its fundamental structural framework but also exhibits enhanced properties suitable for real-time environmental and biomedical sensing applications. The surface composition of the prepared GCN was determined by carrying out the Wide Scan XPS analysis, and the surface functionalities were analysed from their respective Narrow scan analysis. The wide scan spectrum of the prepared GCN (Fig.-2a) exhibits peaks at binding energies (BEs) of 285 eV, 399 eV, and 532 eV, indicating the presence of Carbon (1s), Nitrogen (1s), and Oxygen (1s), respectively.[32] The deconvoluted C (1s) spectrum (Fig.-2b) shows a peak at 288.4 eV, which indicates the presence of sp^2 carbon atoms associated with triazine (C=N bond) correlating well with the results of *T.S. Miller et al.*[33] The presence of surface Oxygen functionalities (C-O/C=O peak at 286.5 eV) observed from the C (1s) narrow scan spectrum of the prepared GCN correlates with the GCN prepared from Urea by *Y. Zheng et al.*[32] The N (1s) narrow scan spectrum (Fig.-2c) was fitted with three peaks at binding energies of 399.7 eV, 399.9 eV, and 400.3 eV corresponding to the pyridinic (C=N), quaternary (sp^3 hybridised nitrogen N-$(C)_3$), and pyrrolic (C-N-H) groups in the GCN structure, respectively. The N-$(C)_3$ units could be attributed to the central Nitrogen atom bridging between three triazine rings in the structure of the prepared GCN.[34] The deconvoluted O (1s) spectrum (Fig.-2d) contains peaks at 532.1 eV and 532.4 eV, indicating the surface functionalities of C=O and C-O, which corroborate with the deconvoluted C (1s) spectrum. The results correlate well with the results of the FT-IR spectrum of the prepared GCN.

The surface defect density ratio (sp^3/sp^2 ratio) calculated from the deconvoluted Narrow scan C (1s) XPS spectrum was found to be 1.2563, which is higher than the structural defect density ratio calculated from Micro-Raman spectral analysis. The XPS spectral results indicate that the functionalization process occurred predominantly at the surface, which enhances the availability of active sites for interaction with analytes. Thus, the present study provides an advancement in designing surface-engineered GCN materials for improved sensing performance compared to conventionally prepared GCNs.

The weight percentage of Carbon, Hydrogen, Nitrogen, Sulfur, and Oxygen (calculated) in the prepared GCN was found to be 33.9, 5.6, 36, 0.8, and 23.7, respectively, from the elemental analysis. The N/C ratio of the prepared GCN is found to be 1.0600, which correlates with the theoretical N/C ratio of GCN (1:33).

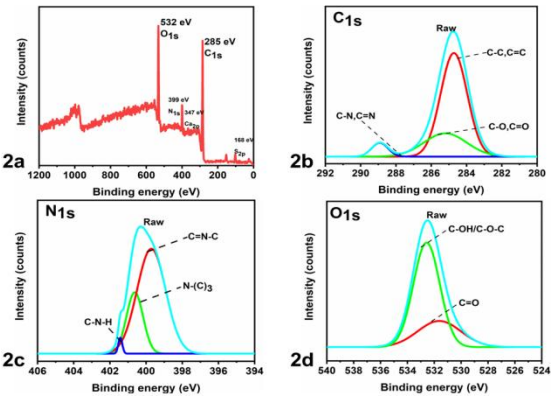

Fig.-(2a): Wide Scan and (2b, 2c & 2d) Deconvoluted C_{1s}, N_{1s} and O_{1s} XPS Spectra of the Prepared GCN

The C/O ratio from CHNS and wide-scan elemental analysis is found to be 1.4304 and 2.1756, respectively. The higher C/O ratio on the surface composition analysis indicates that the presence of Oxygen functionalities (hydroxyl and carbonyl) is higher on the surface of the prepared GCN. It shows that the functionalization happens more on the surface of the prepared GCN, resulting in higher surface defects as indicated by the higher defect density ratio on the surface. The surface functionalization of the prepared GCN can be attributed to the bio-assisted processing of urea at a lower temperature (200°C). It is because functionalization at a lower temperature helps to maintain controlled surface chemistry while preserving its bulk properties. The HR-TEM images of the prepared GCN (Fig.-3a and 3b) indicate the presence of multiple layers in its structure with pores in them. The morphology of the prepared GCN is consistent with that of GCN reported by *Y. Zhang et al.*[25], and *A. Gashi et al.*[35] The Selected Area Diffraction (SAED) Pattern of the prepared GCN (Inset in Fig.-3b) indicates a more crystalline nature, which correlates with the broad peak positioned at 2θ of 27.8º in the PXRD pattern. The combined microstructural and morphological analyses show that a well-defined layered structure GCN can be prepared at lower processing temperatures, contributing to the development of energy-efficient preparation strategies without compromising material quality.

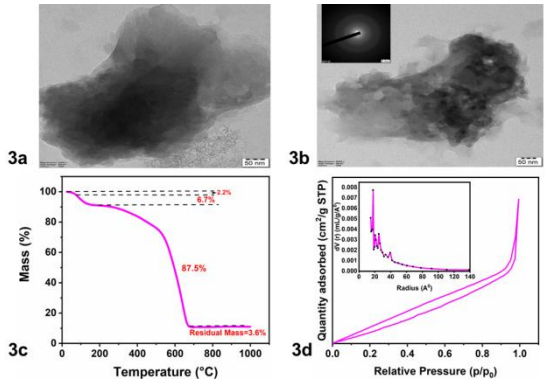

Fig.-(3a and 3b): HR-TEM images (inset: SAED pattern); (3c) Thermogram and (3d) BET Isotherm (inset: BJH plot) of the as-prepared GCN

The thermogram of the prepared GCN (Fig.-3c) shows that the prepared material exhibits very high thermal stability up to 679°C. The initial weight loss of around 97.8°C is due to the elimination of residual water molecules/adsorbed moisture present in the sample. The weight loss between 97.8°C-91°C confirms the presence of Oxygen as adsorbed hydroxyl groups, as evident in the FT-IR spectrum.[26,29] The immediate loss of Oxygen moieties denotes that the Oxygen functionalities are present more on the surface, correlating with the higher surface C/O ratio and sp^3/sp^2 ratio. The major weight loss around 91°C-679°C may be due to the decomposition of the triazine ring units in the structure of the prepared GCN.[31] The TGA results correlate with the results of PXRD, Micro-Raman, and FT-IR in confirming the presence of triazine-based structural units in the prepared GCN. The high thermal stability of the prepared GCN suggests its suitability for real-time sensor application studies in different environmental conditions.

The surface area and pore size distribution of the as-prepared GCN were analysed from the Nitrogen adsorption-desorption isotherms (*Brunauer-Emmett-Teller* (BET) isotherm) and *Barret-Joyner-Halenda* (BJH) pore size distribution curves, respectively. The BET isotherm of the prepared GCN (Fig.-3d) exhibits a Type-III isotherm, which indicates that the GCN possesses weak adsorbate-adsorbent interaction. The BET surface area of the prepared GCN is 90.015 m^2/g, which is higher than the surface area of the GCN (69.6 m^2/g) reported by *Y. Zhang et al.*[25] The BJH plot (Inset in Fig.-3d) shows that the prepared GCN shows a narrow pore size distribution with an average pore diameter of 3.54 nm. From the BJH analysis, it is inferred that the prepared GCN is a mesoporous material. The enhanced surface area and mesoporous structure play an important role in facilitating rapid diffusion and adsorption of target analytes, thereby improving the sensitivity and response time of the sensing system. The preparation of stable, porous, and surface-functionalized GCN for the detection of heavy metal ions supports SDG 6: Clean Water and Sanitation by efficiently monitoring the presence of heavy metal contaminants in environmental systems.

Suggested Mechanism and Structure for the Prepared GCN

On subjecting to thermal carbonisation at a temperature of 200°C, the bioactive organic phytochemicals such as flavonoids, tannins, and polyphenolic compounds in the leaves of *Moringa oleifera* are broken down and undergo a sequence of reactions such as hydrolysis, oligomerisation, condensation, and aromatisation to form aromatic heterocycles such as pyridine, quinoline, quinone, and furan.[12,13] The mixing of aqueous extract of the leaves of *Moringa oleifera* with urea ensures the hydrolysis of urea to cyanuric acid before the thermal treatment, which in turn favours the formation of GCN at the optimised experimental conditions.[33] The cyanuric acid, on subjecting to thermal carbonisation, gets converted into melamine (using self-supported NH_3) to act as the structural units in the formation of GCN.[35] The melamine, on further condensation with the aromatic heterocycles formed from the phytochemicals in the aqueous extract of the leaves of *Moringa oleifera,* may lead to the formation of GCN with enriched surface Oxygen functionalities. Thus, the choice of plant leaf extract for functionalizing the surface of GCN through the thermal carbonisation method facilitated the bio-assisted formation of Oxygen-functionalized GCN at low-temperature conditions.[6,35] The prepared GCN is highly hydrophilic, which may be due to the presence of Oxygen functionalities on the surface of GCN.[36] From the microstructural (PXRD and Micro-Raman) analyses, it can be suggested that the as-prepared GCN has a triazine-based structural units.[37] From the elemental analysis report, it is evident that the amount of Nitrogen and Carbon in GCN is 36% and 33.9%, respectively, which is lower than the theoretical content of Nitrogen and Carbon (60.9% N and 39.1% C, respectively) in GCNs. It may be due to the introduction of a heteroatom, such as oxygen, into the GCN, as identified in FT-IR and XPS spectra, respectively. On comparing the elemental analysis and survey scan spectrum, it is noted that almost 92% of the total Oxygen in the prepared GCN is present mostly on its surface, where its triazine-based structural units are not perturbed by the Oxygen functionalization. Therefore, based on the structural analysis reported by *M. Inagaki et al.,*[38] and the characterisation results of the as-prepared GCN, we propose a representative structure for the prepared GCN (Fig.-4a & 4b):

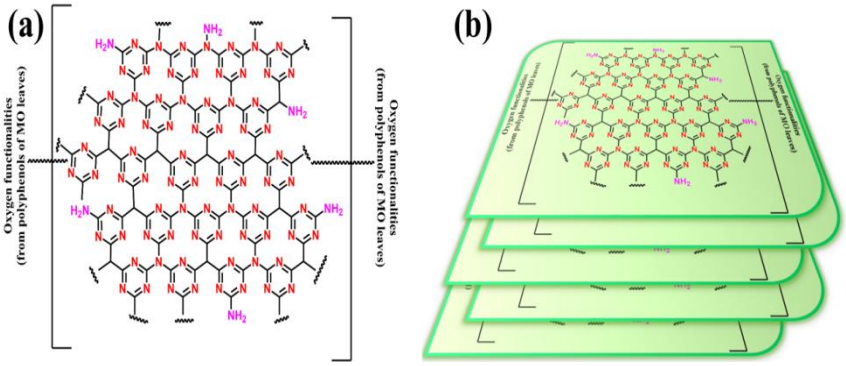

Fig.-(4a): Suggested One-Dimensional View of the Layered Structure of the Prepared GCN[39] and (4b) Representative 3D Image of the Layered Structure

Fluorescent Behaviour of the Prepared GCN

The prepared oxygen-functionalized GCN exhibited an optimum band gap energy of 2.95 eV, enhanced surface defect density and a layered morphology, enabling it to possess improved fluorescence properties.[17] The photoluminescent behaviour was investigated by exciting the sample at different wavelengths from 330 nm to 355 nm at 5 nm intervals (Fig.-5a). The maximum emission intensity was observed at 408 nm under 335 nm excitation. The prepared functionalized GCN shows a blue-shifted emission compared to the reported bulk GCNs, which may be due to the successful exfoliation of the layered structure, as supported by the PXRD and HR-TEM analyses.[15] The excitation wavelength-dependent red-shift of emission from 388 nm to 462 nm suggests the presence of multiple emissive traps generated by surface Oxygen functionalities. This excitation-dependent behaviour differs from the excitation-independent behaviour reported earlier, highlighting the unique defect-mediated optical nature of the prepared GCN.[15]

The role-play of the substrate (prepared GCN) concerning the fluorescence intensity was also investigated. The fluorescence intensity of the prepared GCN follows negative linearity with the increase in the concentration of the GCN solution. The concentration-dependent emission behaviour (Fig.-5b) may be due to the aggregation-induced stacking of triazine units and reduced charge transfer efficiency.[27] The pH-responsive fluorescence behaviour (Fig.-5c) showed maximum intensity at neutral pH, indicating its suitability for physiological and biological environments. The protonation or deprotonation of surface Oxygen functionalities of the prepared leads to this pH-responsive behaviour.[38] The photostability of a fluorophore in the field of biomedical applications is very important. The prepared GCN shows no major photobleaching even after continuous UV irradiation of the sample for 120 minutes (Figure 5d). The prepared GCN shows 97.3% photostability, preferring its high usage as a fluorescent sensor.[40]

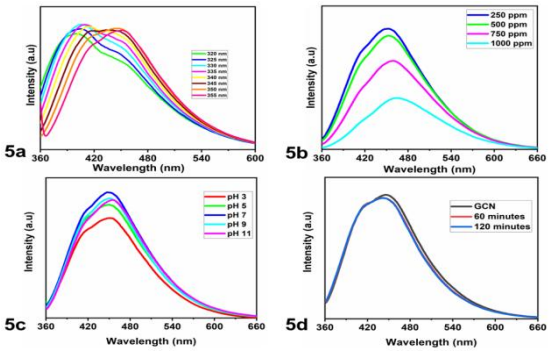

Fig.-(5a): Excitation-dependent (λ_{exc} = 330 nm to 355 nm), (5b) Concentration-dependent (250 ppm to 1000 ppm), (5c) pH-Responsive Fluorescent Behaviour (pH 3 to pH 11); and (5d) Photostability of the Prepared GCN

Efficient Fluorescence Sensing of Heavy Metal Ions - Selectivity of Metal Ions

The detection of environmentally toxic metal ions using Carbon-based fluorescent nanomaterials has gained significant attention in recent days of research. It is because of their excellent solubility, stability, photoluminescence property, ease of preparation, low cost, an abundance of natural sources as precursors, and biocompatibility.[41] The Graphitic Carbon Nitride is an emerging two-dimensional Carbon nanomaterial due to its excellent water solubility, photostability, tunable fluorescence, biocompatibility, and abundance of sustainable precursor sources.[42] In this context, the prepared Oxygen-functionalized GCN provides an important advancement by combining Nitrogen-rich coordination sites with additional surface Oxygen functionalities (C-O and C=O), thereby enhancing metal-ion binding affinity and sensing efficiency. The surface charge of the prepared GCN is found to be -3.65 (negatively charged) from Zeta potential analysis. The negatively charged surface of the prepared GCN favours electrostatic interaction with positively charged metal ions. Therefore, a preliminary screening to determine the selectivity of the prepared GCN (Fig.-6) towards metal ions was carried out using sixteen different metal ions [Cd (II), Zn (II), Fe (II), Cu (II), Ni (II), Mg (II), Pb (II), Mn (II), As (III), Ca (II), Ba (II), Co (II), Cr (VI), Hg (II), and Fe (III)]. Among the different metal ions, the prepared GCN exhibits significant fluorescent quenching (Turn-off fluorescence) towards Cr (VI) ions (Inset in Fig.-6). The higher selective screening capability of

GCN for Cr (VI) ions may be due to the coordination between the Cr (VI) ions and the surface Oxygen functionalities, along with the Nitrogen binding sites (C=N, NH_2) of the prepared GCN.

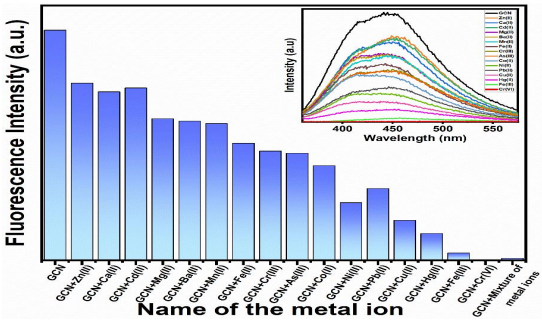

Fig.-6: Heavy Metal Ion Selectivity Study (Inset: Respective Fluorescence spectra) of the Prepared GCN

Fluorescence Sensing of Chromium [Cr (VI)] Ions

Chromium is a transition metal that generally exists in two most stable oxidation states, including the Cr (III) and Cr (VI) forms. Among these two forms, Cr (III) is considered a biologically essential trace element.[43] The Cr (VI) ions enter the ecological system through different industrial sectors such as electroplating, metal finishing, tanning, and textile manufacturing. The Cr (VI) ions are found to be the major contaminant in the tannery industrial effluents with concentrations ranging from 10 mg/L to 1000 mg/L.[44] According to the various national and international standards, including the United States Environmental Protection Agency (US EPA), World Health Organisation (WHO), and Bureau of Indian Standards (BIS), the maximum allowed limit of Cr (VI) ions in drinking water is 0.05 mg/L.[45,46] Therefore, in today's world, the sensitive, rapid, and reliable detection of Cr (VI) ions in aqueous medium is highly important in terms of clean water and sanitation (SDG 6). *M. Rong et al.* (2015)[15], *N. Rahbar et al.* (2018)[47], and *T. Fang et al.* (2016)[48] have reported the use of GCN nanosheets as a fluorescent sensor for the detection of Chromium ions. Based on the results of the heavy metal ion selectivity study, the present study was extended towards optimisation of other experimental conditions (concentration of metal ion solution and influence of pH) for sensing of Cr (VI) ions. In the study, the detection of Cr (VI) ions using the prepared GCN as a fluorescent sensor was carried out with various concentrations of Chromium ranging from 10 mM to 0.03 mM. The change in the emission intensity of the GCN solution upon addition of Cr (VI) ions was recorded. The optimum concentration of Cr (VI) ions for the complete quenching of the emission intensity of GCN was found to be 10 mM. The sensing efficiency of the GCN towards Cr (VI) ions was explored under acidic, neutral, and alkaline pH conditions. The fluorescence sensing of Cr (VI) ions by GCN under pH=3, 7 and 11 is shown in Fig.-7a, 7b and 7c, respectively. It was found that the pH of the medium has no remarkable influence on the optimum concentration of Cr (VI) ions, which also indicates the stability of the prepared GCN as a selective sensor for Cr (VI) ions.

The efficiency of fluorescence quenching was quantitatively evaluated through the *Stern-Volmer* relationship.[49]

$$\frac{I_0}{I} = 1 + K_{SV}[Q]$$

Where I_0 and I are the fluorescence intensities of the GCN in the absence and presence of quencher (metal ion), K_{SV} is the *Stern-Volmer* constant/quenching constant/slope of the linear fit, and [Q] is the concentration of quencher (metal ion).

The *Stern-Volmer* Plot (Fluorescence intensity vs. Concentration of Cr (VI) ion) for the pH 7 (Fig.-7d) exhibits a positive linear relationship in the concentration range of 0.03 mM to 0.5 mM with a correlation coefficient of $R^2 = 0.9964$. The limit of detection was calculated via the following equation,

$$Limit\ of\ Detection = \frac{3\sigma}{m}$$

Where σ is the standard deviation of the fluorescent signals of the prepared GCN (n=6), and m is the slope of the linear fit of the *Stern-Volmer* plot.

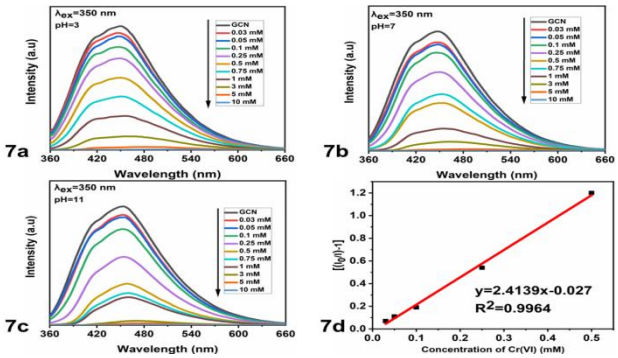

Fig.-(7a, 7b and 7c): Fluorescence Sensing of Hexavalent Chromium Ions at pH 3, 7 & 11; and (7d) *Stern-Volmer* Plot of GCN-Cr (VI) Ions Sensing Study at pH 7

The Limit of Detection of Cr (VI) ions using the prepared GCN was found to be 59 µM. To date, the detection limit of Cr (VI) ions by Carbon-based zero-dimensional and two-dimensional materials prepared by *S. Bhatt et al.* (2018)[50], *S. Ebrahim et al.* (2020)[51], and *J. Yadav et al.* (2024)[52] is found to be in the range of 1.6 µM to 0.184 µM. These sensors were processed at temperatures above 500°C in the form of nanocomposites.[51,52] But the present study is unique in the fact that the sensor, which is used for the detection of Cr (VI) ions, is only the prepared Oxygen functionalized GCN, that too prepared at a lower processing temperature. Though the detection limit of the prepared GCN exceeds the permissible limit of 0.05 mg/L of Cr (VI) ions in drinking water, it matches the concentration of Cr (VI) ions (above 10 mg/L) in industrial effluents. It indicates that under the given experimental conditions, the prepared GCN can be an effective fluorescent sensor for detecting the Cr (VI) ions in the industrial effluents for environmental applications.

Possible Fluorescence Sensing Mechanism

The fluorescence lifetime of the as-prepared GCN is found to be 4.34 ns (nano seconds), which decreased to 3.95 ns upon adding Cr (VI) ions, respectively. The change in fluorescence lifetime and the linear *Stern-Volmer* plot indicate that the mechanism of fluorescence quenching followed by the prepared GCN while detecting the Cr (VI) ions is dynamic.[15] The fluorescent sensor following dynamic quenching offers significant advantages by reducing the interference from other substances in the system (ensuring high selectivity) and allowing for accurate quantitative analysis (providing high sensitivity).[53] To study the quenching mechanism in detail, the energy levels of the prepared GCN were determined. The highest occupied molecular orbital (HOMO) and lowest occupied molecular orbital (LUMO) of the prepared GCN are calculated as per the reports of *C. Liu et al.* (2021).[54]

$$E_{HOMO} = -\left(E_{ox} + 4.4\right) eV \quad (1)$$

$$E_{LUMO} = -\left(E_{red} + 4.4\right) eV \quad (2)$$

$$E_{HOMO} = E_{LUMO} - E_g \quad (3)$$

Where E_{ox} and E_{red} are the oxidation and reduction potential of the prepared GCN, respectively.

The value of reduction potential and the direct band gap energy of the prepared GCN were found to be 0.33 eV and 2.95 eV from the Cyclic Voltammogram (Supplementary Fig.-1) and UV-Visible absorption spectrum (Fig.-1c), respectively. Then, using equations (2) and (3), the HOMO and LUMO of the prepared GCN are determined as -4.73 eV and -7.63 eV, respectively. Based on the redox potential values of metal ions from the Electrochemical series, the HOMO/LUMO of metal ions were calculated.[55] It is observed that the HOMO/LUMO band gap of the as-prepared GCN overlaps with the HOMO of Hg (II) [-5.5 eV], Cu (II) [-4.74 eV], Pb (II) [-4.27 eV], Co (II) [-4.12 eV], Fe (III) [-4.36 eV], Ni (II) [-4.15 eV], and Cr (VI) [-5.73 eV] indicating that the electron-transfer between the GCN with the metal ions is

energetically allowed. Thus, the fluorescence quenching (turn-off fluorescence) of the as-prepared GCN may be due to the process of photo-induced electron transfer mechanism (a type of dynamic quenching) that occurs from the LUMO of the fluorophore (GCN) to the HOMO of the quencher [(Cr (VI) ions].[42]

Detection of Cr (VI) Ions in Real-Time Samples

Detection of Cr (VI) Ions in Tannery Industrial Effluent

The satisfactory performance of the prepared GCN as a fluorescent sensor was further explored for the detection of Cr (VI) ions in tannery industrial effluent as a pilot study. The study was followed through standard ICP-OES method. The tannery industrial effluent used in the study was simulated as per the reports of *M. Chowdhury et al.* (2015),[23] and discussed earlier in Section 2.5.1. The concentration of Cr (VI) ions in the tannery effluent was determined using a calibration graph of fluorescence intensity of the prepared GCN vs known concentration of 5 mM to 1 mM of Cr (VI) ions, and is given in the Supplementary Fig.-2 (a). The amount of Cr (VI) ions detected in the prepared tannery industrial effluent through the present study and the ICP-OES method was 1.5 mM and 1.7 mM, respectively. It is observed that a very good correlation exists between the Cr (VI) ions detected through the present study and the ICP-OES method, with an error percentage of less than one. Therefore, the results of the study confirm the high reliability and applicability of the prepared GCN as a fluorescent sensor for detecting the Cr (VI) ions in industrial effluents.

Detection of Cr (VI) Ions in Commercial Food-Grade Turmeric Samples

The study was further extended for the detection of Chromium (VI) adulteration in the turmeric powders, one of the commonly used spices globally. To enhance the yellow colour appearance of the commercial turmeric powders, they are largely adulterated with toxic chemicals like metanil yellow dye and lead chromate.[25] Three different brands of food-grade turmeric samples were purchased, and their solutions was prepared in the ratio of 1:10 (w/v). The concentration of Cr (VI) ions in the turmeric powders was determined using a calibration graph of fluorescence intensity of the prepared GCN vs known Cr (VI) concentrations of 200 μM to 500 μM. The corresponding calibration graph is given in the Supplementary Fig.-2 (b). In the study, it was found that the purchased commercial food-grade turmeric powders contain Chromium in the range of 3.1-5.3 μg/g. The study exhibits a detection limit of $3x10^{-4}$ % (w/w) using the prepared GCN as a fluorescent sensor for Cr (VI) ions in turmeric powders. The study reports by *R. Paranthaman et al.* (2021)[56], *S.W. Erasmus et al.* (2021)[57], and *T. Kumar et al.* (2022)[58] utilised the PXRD, Raman and Atomic Emission spectroscopic methods in detecting the Chromium adulteration in turmeric samples, and achieved a detectable limit of 0.5% (w/w), 0.5% (w/w) and 0.7% (w/w), respectively. It shows that under the given experimental conditions, the fluorescence sensing method using the prepared GCN as a sensor is found to be a good model compared to the reported X-ray diffraction and spectroscopic methods. Therefore, the future exploration of the study can focus on enhancing the detectable limit of the prepared GCN by tuning its surface functionalities on par with the standard techniques like ICP-OES and ICP-MS.

CONCLUSION

The present study reported a simple, low-temperature, and bio-assisted method for the preparation of Oxygen functionalized Graphitic Carbon Nitride using urea and extract of the leaves of *Moringa oleifera*. The layered structure of the prepared GCN was confirmed from its microstructural and morphological analyses. The presence of surface Oxygen functionalities enhances its surface-active principles, leading to improved fluorescence behaviour with enhanced photostability. The prepared functionalized GCN exhibits tunable fluorescent behaviour. The fluorescent behavior of the prepared GCN was further extended for the detection of Chromium [Cr (VI)] ions through a fluorescence sensing. The study successfully detected the presence of Cr (VI) ions as a pollutant in tannery industrial effluent and as an adulterant in turmeric powders of the food industry using the prepared GCN as a fluorescent sensor. The fluorescence quenching mechanism may be due to the electron transfer, as supported by the lifetime analysis. The present study can be further taken up for the fabrication of a fluorescent sensor by tuning the surface functionalities and improving sensitivity comparable to standard analytical techniques. Ultimately, the study provided a cost-effective and sustainable approach for developing advanced

functional nanomaterials for environmental sensing, which aligns with SDG-6 by contributing to improved water quality and environmental safety.

ACKNOWLEDGMENTS

The authors acknowledge and thank the Directorate of Collegiate Education, Government of Tamil Nadu, for funding the Research (Ref. No: Rc. No. 00160/L/2022 Dated 14.11.2023), and the PG and Research Department of Chemistry, Ethiraj College for Women, for their support and encouragement.

CONFLICT OF INTERESTS

The authors declare that there is no conflict of interest.

AUTHOR CONTRIBUTIONS

The present work is related to *SDG-6:Clean Water and Sanitation*. All the authors contributed significantly to this manuscript, participated in reviewing/editing and approved the final draft for publication. The research profile of the authors can be verified from their ORCID ids, given below:

S. Sudhaparimala http://orchid.org/0000-0002-4608-0419
C. Valarmathy http://orchid.org/0009-0008-2324-5699

Cite this article as: S. Sudhaparimala and C. Valarmathy, *Rasayan J. Chem.*, 19(3), 1539-1552(2026), https://doi.org/10.31788/RJC.2026.1939587

REFERENCES

1. L.H. Madkour, *International Research Journal of Basic Clinical Studies,* **8,** 1(2023), https://doi.org/10.14303/irjbcs.2023.48
2. J. Zhang, M. Chen, X. Ren, W. Shi, T. Yin, T. Luo, Y. Lan, X. Li, and L. Guan, *RSC Advances,* **13**, 27714(2023), https://doi.org/10.1039/D3RA05031A
3. A.P. Drdanová, T.E. Krajčovičová, M. Gál, K. Nemčeková, Z. Imreová, J. Ryba, M. Naumowicz, T. Homola, T. Mackuľak, and V. Svitková, *International Journal of Molecular Sciences,* **25**, 7634(2024), https://doi.org/10.3390/ijms25147634
4. P. Praus, A. Smýkalová, K. Foniok, V. Novák, and J. Hrbáč, *Journal of Environmental Chemical Engineering,* **9**, 105498(2021), https://doi.org/10.1016/j.jece.2021.105498
5. M. Singhal, S. Jangir, S. Upadhyay, and D.S. Rajawat, *Discover Chemistry,* **1**, 64(2024), https://doi.org/10.1007/s44371-024-00055-1
6. T. Fidan, M. Torabfam, Q. Saleem, C. Wang, H. Kurt, M. Yüce, J. Tang, and M.K. Bayazit, *Advanced Energy and Sustainability Research,* **2**, 2000073(2021), https://doi.org/10.1002/aesr.202000073
7. Y.P. Sun, W. Ha, J. Chen, H.Y. Qi, and Y.P. Shi, *Trends Analytical Chemistry,* **84**, 12(2016), https://doi.org/10.1016/j.trac.2016.03.002
8. F. Ma, Y. Ji, B. Liu, J. Wang, B. Zhou, G. Zhen, F. Long, and Z. Zou, *Materials Research Express,* **7**, 115002(2020), https://doi.org/10.1088/2053-1591/abc4b6
9. L.H. Amorin, V.Y. Suzuki, N.H. de Paula, J.L. Duarte, M.A.T. da Silva, and C.A. Taft, *New Journal of Chemistry,* **43**, 13647(2019), https://doi.org/10.1039/C9NJ02702E
10. Z. Islam, S.R. Islam, F. Hossen, K. Mahtab-ul-Islam, M.R. Hasan, and R. Karim, *International Journal of Food Science,* **1**, 6627265(2021), https://doi.org/10.1155/2021/6627265
11. B. Moyo, P.J. Masika, A. Hugo, and V. Muchenje, *African Journal of Biotechnology,* **10**, 12925(2011), https://doi.org/10.5897/AJB10.1599
12. S. Lin, J. Simal-Gandara, H. Cao, and J. Xiao, *Current Research in Food Science,* **6**, 100509(2023), https://doi.org/10.1016/j.crfs.2023.100509
13. S. Lin, H. Zhang, J. Simal-Gandara, K.W. Cheng, M. Wang, H. Cao, and J. Xiao, *Food Chemistry,* **386**, 132747(2022), https://doi.org/10.1016/j.foodchem.2022.132747

14. B. Saha, A. Amine, and F. Verpoort, *Chemistry Africa,* **5**, 1779(2022), https://doi.org/10.1007/s42250-022-00443-z
15. M. Rong, L. Lin, X. Song, Y. Wang, Y. Zhong, J. Yan, Y. Feng, X. Zeng, and X. Chen, *Biosensors and Bioelectronics,* **68**, 210(2015), https://doi.org/10.1016/j.bios.2014.12.024
16. H.N.M.E. Mahmud, A.O. Huq, and R. binti Yahya, *RSC Advances,* **6**, 14778(2016), https://doi.org/10.1039/C5RA24358K
17. P. Babu, H. Park, and J.Y. Park, *Surface Science and Technology,* **1**, 29(2023), https://doi.org/10.1007/s44251-023-00026-1
18. C. Valarmathy and S. Sudhaparimala, *International Journal of Nanoscience and Nanotechnology*, **19**, 263(2023), http://dx.doi.org/10.22034/ijnn.2023.2006835.2398
19. R.D. Jayanti, N. Rahmawati, E.S. Wulaningtyas, N.A. Hastuti, S. Winarsih, and A.G. Ningrum, *World Journal of Advanced Research and Reviews,* **23**, 2245(2024), https://doi.org/10.30574/wjarr.2024.23.3.2786
20. C. Valarmathy and S. Sudhaparimala, 2024, Low temperature preparation of Graphitic Carbon Nitride from *Moringa oleifera* leaves-Screening of fluorescence and anti-oxidant property, in: Proceedings of International Conference on Advanced Functional Materials and Devices, Published by Nanotechnology Research Centre, SRM University, Kattankulathur, pp. 807.
21. M. Nigam, S. Rajoriya, S.R. Singh, and P. Kumar, *Journal of Environmental Chemical Engineering,* **7,** 103188(2019), https://doi.org/10.1016/j.jece.2019.103188
22. J.E. Forsyth, D. Mistree, E. Nash, M. Angrish, and S.P. Luby, *Science of the Total Environment,* **949,** 175003(2024), https://doi.org/10.1016/j.scitotenv.2024.175003
23. M. Chowdhury, M.G. Mostafa, T.K. Biswas, A. Mandal, and A.K. Saha, *Environmental Process,* **2**, 173(2015), http://dx.doi.org/10.1007/s40710-015-0065-7
24. T.D. Burchell, Carbon Materials for Advanced Technologies, *Elsevier,* p.22,23(1999), https://doi.org/10.1016/b978-0-08-042683-9.x5000-6
25. Q. Zhuang, L. Sun, and Y. Ni, *Talanta,* **164**, 458(2017), https://doi.org/10.1016/j.talanta.2016.12.004
26. Y. Zhang, J. Liu, G. Wu, and W. Chen, *Nanoscale,* **4**, 5300(2012), https://doi.org/10.1039/C2NR30948C
27. A. Sewnet, E. Alemayehu, M. Abebe, D. Mani, S. Thomas, and N. Kalarikkal, *Nanomaterials,* **13**, 762(2023), https://doi.org/10.3390/nano13040762
28. R. Tang, R. Ding, and X. Xie, *Water Science and Technology,* **78**, 1023(2018), https://doi.org/10.2166/wst.2018.361
29. P. Choudhary, A. Bahuguna, A. Kumar, S.S. Dhankhar, C.M. Nagaraja, and V. Krishnan, *Green Chemistry,* **22**, 5084(2020), https://doi.org/10.1039/D0GC01123A
30. Mark Wall, *The Raman Spectroscopy of Graphene and the Determination of Layer Thickness,* Madison, WI, USA: Thermo Fisher Scientific.
31. A.M. Bernhard, D. Peitz, M. Elsener, A. Wokaun, and O. Kröcher, *Applied Catalysis B: Environment and Energy,* **115,** 129(2012), https://doi.org/10.1016/j.apcatb.2011.12.013
32. Y. Zheng, Z. Zhang, and C. Li, *Journal of Photochemistry and Photobiology A: Chemistry,* **332**, 32(2017), https://doi.org/10.1016/j.jphotochem.2016.08.005
33. T.S. Miller, A.B. Jorge, T.M. Suter, A. Sella, F. Corà, and P.F. McMillan, *Physical Chemistry Chemical Physics,* **19**, 15613(2017), https://doi.org/10.1039/C7CP02711G
34. H. Dai, X. Gao, E. Liu, Y. Yang, W. Hou, L. Kang, J. Fan, and X. Hu, *Diamond and Related Materials,* **38**, 109(2013), https://doi.org/10.1016/j.diamond.2013.06.012
35. A. Gashi, J. Parmentier, P. Fioux, and R. Marsalek, *Chemistry-A European Journal,* **28**, e202103605(2022), https://doi.org/10.1002/chem.202103605
36. Y.A. El-Reash, E.A. Ghaith, O. El-Awady, F.K. Algethami, H. Lin, and E.A. Abdelrahman, *Journal of Analytical Science and Technology,* **14**, 16(2023), https://doi.org/10.1186/s40543-023-00379-0
37. Z. Zhao, Y. Ma, J. Fan, Y. Xue, H. Chang, Y. Masubuchi, and S. Yin, *Journal of Alloys and Compounds,* **735,** 1297(2018), https://doi.org/10.1016/j.jallcom.2017.11.033
38. M. Inagaki, T. Tsumura, T. Kinumoto, M. Toyoda, *Carbon,* **141**, 580(2019), https://doi.org/10.1016/j.carbon.2018.09.082

39. X. Guan, Z. Li, X. Geng, Z. Lei, A. Karakoti, and T. Wu, *Small,* **19**, 2207181(2023), https://doi.org/10.1002/smll.202207181
40. D. Ceballos-Ávila, I. Vazquez-Sandoval, F. Ferrusca-Martínez, and A. Jiménez-Sánchez, *Biosensors and Bioelectronics,* **264,** 116638(2024), https://doi.org/10.1016/j.bios.2024.116638
41. R. Roy, A.R. Chacko, T. Abraham, B.K. Korah, B.K. John, M.S. Punnoose, C. Mohan, and B. Mathew, *Chemistry Select,* **7**, e202200876(2022), https://doi.org/10.1002/slct.202200876
42. X. Guan, Z. Li, X. Geng, Z. Lei, A. Karakoti, and T. Wu, *Small,* **19**, 2207181(2023), https://doi.org/10.1002/smll.202207181
43. A. Hussen, *Asian Journal of Basic Science & Research,* **3**, 69(2021), http://dx.doi.org/10.38177/AJBSR.2021.3106
44. Q. Jin, M. Dai, X. Zhan, S. Wang, and Z. He, *Journal of Alloys and Compounds,* **922**, 166268(2022), https://doi.org/10.1016/j.jallcom.2022.166268
45. H.A. El-Gawad, G.K. Hassan, K.M. Aboelghait, W.H. Mahmoud, R.M. Mohamed, and A.A. Afify, *Scientific Reports,* **13**, 19597(2023), https://doi.org/10.1038/s41598-023-46848-9
46. B.M. Reif and B.P. Murray, Chromium Toxicity, StatPearls Publishing, p.2-14(2024).
47. N. Rahbar, Z. Salehnezhad, A. Hatamie, and A. Babapour, *Microchimica Acta*, **185**, 101(2018), https://doi.org/10.1007/s00604-017-2615-3
48. T. Fang, X. Yang, L. Zhang, and J. Gong, *Journal of Hazardous Materials,* **312**, 106(2016), https://doi.org/10.1016/j.jhazmat.2016.03.046
49. A. Sachdev and P. Gopinath, *Analyst,* **140**, 4260(2015), https://doi.org/10.1039/C5AN00454C
50. S. Bhatt, M. Bhatt, A. Kumar, G. Vyas, T. Gajaria, and P. Paul, *Colloids and Surfaces B: Biointerfaces,* **167**, 126(2018), https://doi.org/10.1016/j.colsurfb.2018.04.008
51. S. Ebrahim, A. Shokry, M.M. Khalil, H. Ibrahim, and M. Soliman, *Scientific Reports,* **10**, 13617(2020), https://doi.org/10.1038/s41598-020-70678-8
52. J. Yadav, M. Rani, and U. Shanker, *New Journal of Chemistry,* **48**, 9376(2024), https://doi.org/10.1039/D4NJ00814F
53. B.T. Huy, D.T. Thangadurai, M. Sharipov, N.N. Nghia, N. Van Cuong, and Y.I. Lee, *Microchemical Journal,* **179**, 107511(2022), https://doi.org/10.1016/j.microc.2022.107511
54. C. Liu, F. Zhang, J. Hu, W. Gao, and M. Zhang, *Frontiers in Chemistry,* **8**, 605028(2021), https://doi.org/10.3389/fchem.2020.605028
55. J.H. He, Y.Y. Cheng, T. Yang, H.Y. Zhou, and C.Z. Huang, *Analytica Chimica Acta,* **1035**, 203(2018), https://doi.org/10.1016/j.aca.2018.06.053
56. R. Paranthaman, J.A. Moses, and C. Anandharamakrishnan, *Food Control,* **126**, 107992(2021), https://doi.org/10.1016/j.foodcont.2021.107992
57. S.W. Erasmus, L. van Hasselt, L.M. Ebbinge, and S.M. van Ruth, *Food Control,* **121**, 107714(2021), https://doi.org/10.1016/j.foodcont.2020.107714
58. T. Kumar, A.K. Rai, A. Dwivedi, R. Kumar, M. Azam, V. Singh, N. Yadav, and A.K. Rai, *Atoms,* **10**, 91(2022), https://doi.org/10.3390/atoms10030091

[RJC-9587/2025]